

RECURRENT NEURAL NETWORKS FOR AIR-FUEL RATIO ESTIMATION AND CONTROL IN SPARK-IGNITED ENGINES

Arsie, I., Di Iorio, S., Pianese, C., Rizzo, G., Sorrentino, M.

*Department of Mechanical Engineering, University of Salerno
Fisciano, 84084, Italy*

Abstract: The paper focuses on the experimental identification and validation of recurrent neural network (RNN) models for air-fuel ratio (AFR) estimation and control in spark-ignited engines. Suited training procedures and experimental tests are proposed to improve RNN precision and generalization in predicting AFR transients for a wide range of operating scenarios. The reference engine has been tested by means of an integrated system of hardware and software tools for engine test automation and control strategies prototyping. The simulations performed on the test-sets show the ability of the RNN to reproduce the target patterns with satisfactory accuracy. Finally, real time implementation of RNN has been accomplished by developing and testing an inverse neural network controller acting on the injection time to limit AFR excursions from stoichiometry.
Copyright © 2008 IFAC.

Keywords: Nonlinear dynamic modeling, Neural networks, Engine Modeling, Engine Control, Diagnostics.

1. INTRODUCTION

Air-fuel ratio is a key challenge and keeps being an open problem for the engine control community. Since the eighties, the transition from carburetor to electronically controlled injection system motivated the researcher to concentrate on this topic. Proper control of air-fuel ratio is greatly beneficial to the three way catalyst performance in both steady and transient operations. Therefore this control task plays a fundamental role in limiting exhaust emissions in SI engines.

Despite the considerable efforts made, the more stringent environmental regulations imposed throughout the world make the achievement of satisfactory conversion efficiency still an ambitious goal. Furthermore, the engine control system (ECS) designers have to deal with the on board diagnostics (OBD) requirements, introduced since 1996 in US and later in Europe. This represents a more critical goal in the field of automotive control, since it requires to continuously monitor all powertrain components to prevent critical faults with respect to exhaust emissions.

AFR control currently relies on a mean value engine model representation. The outstanding works of Aquino (1981) and Hendricks and Sorenson (1991) represent the foundation of the actual AFR controller implemented on mass market vehicles. Such a controller estimates in a feedforward way the air flow rate at the injector location, providing the right amount of fuel to be delivered with the appropriate time dependence. The implementation of this control within a feedback compensation loop allows further correction of the injection time based on the measurements performed by the oxygen sensor.

Despite their accuracy, mean value models have some significant limitations, such as the high experimental burden requested for parameters identification and the

intrinsic non-adaptive features. To overcome the latter problem, adaptive methodologies have been proposed in order to estimate the states and tune the parameters making use of real-time measurements (e.g. observers, Kalman filters) (Arsie et al., 2003; Locatelli et al., 2006; Powell et al., 1998; Turin and Geering, 1994) or robust control methodologies (e.g. H_∞ control) (Vigild et al., 1999). On the other hand, the AFR signal delay represents a very critical issue to be overcome to improve the performance of the closed-loop control strategies (Powell et al., 1998; Choi and Hedrick, 1998).

A promising solution for approaching these problems is given by Neural Networks based black-box models, which have high mapping capabilities and guarantee a good generalization even with a reduced set of identification data. Moreover, the possibility of implementing adaptive training procedures allows to take into account the influence of exogenous effects on control performance (Haykin, 1999; Patterson, 1995; Nørgaard et al., 2000).

Some examples of NN models for automotive application have been proposed in the literature for engine control (Shayler et al., 1996), diagnostics (Ortmann et al., 1998; Capriglione et al., 2003), sensor data fusion and pattern recognition (Patterson, 1995), with satisfactory robustness even in presence of noisy data. Neural networks have also been proven useful for modeling nonlinear dynamic systems introducing feedback connections in a recursive computational structure (i.e. RNN). In the engine modeling and control fields, of particular interest are the contribution of Colin et al. (2007), Tan and Saif (2000) and Dovifaaz et al. (1999).

In this work, RNN models are trained and tested to simulate both forward and inverse nonlinear dynamics of the intake manifold air-fuel flow. Suited training

procedures are proposed to develop RNN models of AFR excursions for both diagnostics and control applications.

2. POTENTIALITIES OF RNN FOR AFR ESTIMATION

The actual state of the art of AFR control relies on both feedforward and feedback control strategies. The base injection pulse is computed as function of desired AFR, engine speed, manifold pressure, throttle opening, feedback exhaust oxygen sensor and a number of factors to account for changes in ambient conditions, battery voltage and engine thermal state. During transient operation, in order to compensate for the different dynamic response of air and fuel path due to the wall wetting phenomenon, the base injected fuel is compensated by a feedforward controller. This latter is usually based on a mean value model (MVM) according to the approach originally proposed by Aquino (1981). The MVM parameters are computed accounting for the influence of engine operation and thermal state on fuel wall wetting and engine breathing, respectively. The output of the MVM-based feedforward controller is then further corrected by a closed loop control task and a long term fuel trim. The former is based on a PI controller aimed at keeping the AFR measured by the exhaust oxygen sensor as close as possible to the desired value, as addressed by the catalyst control strategies (Yasuri et al., 2000). Similarly to the MVM parameters, the PI gains are stored in look-up tables to account for their dependence on engine operating conditions. Long term fuel trim is intended to compensate for imbalance and/or offset in the AFR measurement due to exogenous effects, such as canister purge events, engine wearing, air leaks in the intake manifolds, etc. (Yoo et al., 1999).

The control strategy described above has been well established in the automotive industry for long time, thanks to its good performance during both steady and transient conditions. Nevertheless, the more stringent regulations imposed in the last years (i.e. OBD and Low Emission Vehicles) have pushed car manufacturers towards further developing the actual control strategies implemented on commercial ECU. On the other hand, design burden has increased and the reduction of calibration efforts, required to develop the parameter maps and to improve the feedback control performance, has become a stringent need.

Recurrent Neural Network, whose modeling features are presented in the following section, have significant potential to face the issues associated with AFR control. The authors themselves showed how an inverse controller made of two RNNs, simulating both forward and inverse intake manifold dynamics, is suitable to perform the feedforward control task (Arsie et al., 2004 and 2006a). Network training can be fulfilled using only one highly-informative data-set, thus reducing the calibration effort with respect to Aquino-based approaches. Moreover, the opportunity of adaptively modifying network parameters allows accounting for other exogenous effects, such as change in environmental conditions, construction tolerances and engine wear.

The suitability of RNN AFR estimators to improve feedback control is twofold. On one hand, they can be used in virtual sensing applications, such as the prediction of AFR in cold-start phases. RNN training during cold-start can be performed on the test-bench off-line, by pre-heating the lambda sensor before turning on the engine. On the other hand, proper post-processing of training data enables to predict AFR excursions without the delay between injection (at intake port) and measuring (in the exhaust) events, thus being suitable in the framework of sliding-mode closed-loop control tasks (Yasuri et al., 2000; Choi and Hedrick, 1998). In such an application the feedback provided by a UEGO lambda sensor should be used to adaptively modify the RNN estimator to take into account exogenous effects.

Moreover, RNN-based estimators are well suited for diagnosis of injection/air intake system and lambda sensor failures (Maloney, 2001). Differently from control applications, in this case it is envisioned that the AFR prediction includes the measuring delay.

Main contributions of the present paper are numerical/experimental methodologies aimed at improving RNN accuracy. Well-known problems associated with network training, such as data overfitting and overtraining, are addressed. Moreover, an error-based procedure is followed in order to identify the measuring delay and, eventually, removing it depending on the specific application the AFR estimator is developed for. Finally, an example of real-time implementation of RNN for AFR control is given, namely the development of an inverse RNN acting as a compensator to limit AFR excursions from stoichiometry.

3. RECURRENT NEURAL NETWORK FOR AFR DYNAMICS MODELING

3.1 RNN architecture

The RNNs are derived from the static multi layer perceptron feed forward (MLPFF) networks by adding feedback connections among the neurons, thus introducing a dynamic effect in the computational system. Therefore, due to the non-linear mapping features of the MLPFFs, the RNNs are suitable for black-box non-linear dynamic modeling (Patterson, 1995; Haykin, 1999).

Depending upon the feedback typology, which can either involve all the neurons or only the ones located in the output and input layers, RNNs are classified into global, local or external recurrent neural networks (Haykin, 1999). The latter being the class used in this work with one hidden layer of nodes. The sketch of Fig. 1 gives the schematic representation of the following general form:

$$\hat{y}(t, \theta) = F[\hat{y}(t-1, \theta), \dots, \hat{y}(t-n, \theta), u(t-1), \dots, u(t-m), x(t-1), \dots, x(t-m)] \quad (1)$$

where \hat{y} , u and x are the output, control and external input variables, respectively; while θ is the vector of parameters (weights). The indices n and m are set once the lag spaces of both external input x and feedback variable \hat{y} have been fixed. In Fig. 1 the lag space values are set equal to 2. The terms in square brackets of Eq. (1) compose the RNN regressors vector, which is representative of the past process dynamics. F is the non-linear mapping operation

performed by the neural network. The RNN described above is known in the literature as nonlinear output error model (NOE) (Nørgaard et al., 2000).

In the current application, as the dynamic processes affecting AFR transient response depend on both air and fuel dynamics, the output, control and external input variables are, respectively:

$$\begin{aligned} \hat{y} &= AFR \\ u &= t_{inj} \end{aligned} \quad (2)$$

$$x = [rpm, p_{man}]$$

Therefore, the NOE RNN resulting from Eq. (1) will be:

$$\begin{aligned} A\hat{F}R(t, \theta) = F[&A\hat{F}R(t-1, \theta), \dots, A\hat{F}R(t-n, \theta), t_{inj}(t-1), \\ &\dots, t_{inj}(t-m), rpm(t-1), \dots, rpm(t-m), \\ &\dots, p_{man}(t-1), \dots, p_{man}(t-m)] \end{aligned} \quad (3)$$

It is worth to note that the output feedbacks in the regressors vector (i.e. $A\hat{F}R$ in Eq. (3)) are simulated by the network itself, thus the RNN does not require any AFR measurement as feedback to perform the online estimation. This represents a very appealing feature that makes the NOE structure a suitable solution for AFR estimation when the oxygen sensor does not guarantee an accurate measurement, as it happens during cold start phases.

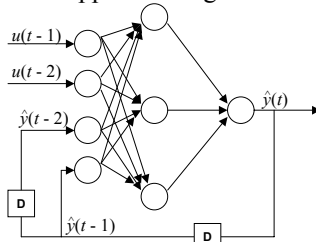


Fig. 1. Structure of NOE RNN with one input variable, one output, one hidden layer and two output delays D.

3.2 RNN training methodologies

Network training is performed by minimizing a cost function estimated as function of the mean squared error (MSE). A weight regularization term is added to improve model generalization:

$$E(\theta) = \frac{1}{2N} \sum_{t=1}^N (\hat{y}(t|\theta) - y(t))^2 + \frac{1}{2N} \cdot \theta^T \cdot \alpha \cdot \theta \quad (4)$$

where α is a scalar and represents the weight decay. The above function minimization can be conducted in either a batch or an adaptive way. The former is usually preferred at the initial development stage, whereas the latter is greatly beneficial to online RNN implementation as it allows to adapt network weights to the exogenous variations of the controlled/simulated system.

A proper design of RNN can be ensured by appropriately addressing the following issues (Sorrentino et al., 2007): *i*) generate a training data set extensive enough to guarantee acceptable generalization of the knowledge retained in the training examples, *ii*) select the proper stopping criteria to prevent overtraining and *iii*) define the network structure with the minimum number of weights.

As far as the impact of point *i*) concerns the current application, AFR dynamics can be well learned by the RNN estimator once the trajectories of engine state

variables (i.e. manifold pressure p_{man} and engine speed [rpm]) described in the training-set are informative enough. This means that the training experiments on the test-bench are to be performed in such a way as to cover most of the engine working domain. Furthermore a proper description of both low- and high-frequency dynamics is necessary. Thus the required experimental profile is obtained by alternating steady operations of the engine with both smooth and sharp acceleration/deceleration maneuvers.

Point *ii*) can be approached by introducing the early-stopping method as stopping criterion. This technique consists in interrupting the search for the minimum, once the MSE computed on a data-set different from the training one stops decreasing. Finally, point *iii*) is addressed by referring to a previous paper (Arsie et al., 2006b), in which a trial and error analysis was performed to select the optimal network architecture in terms of hidden nodes and lag space. Although some theories about MLPFF network sizing are addressed in the specific literature (Kolmogorov, 1965), finding the best architecture for recurrent neural network is a more challenging task due to the presence of feedback connections and past input values (Nørgaard et al., 2000). Therefore, the recourse to an heuristic error-based approach is suitable to satisfactorily fulfill point *iii*).

4. EXPERIMENTAL SET-UP

The RNN AFR estimator has been trained and tested vs. transient data sets measured on the engine test bench at the University of Salerno.

The experiments have been carried out on a commercial engine, 4 cylinders, 1.2 liters, with Multi-Point injection. The test bench is equipped with a Borghi & Saveri FE-200S eddy current dynamometer. A data acquisition system, based on National Instruments cards PCI MIO 16E-1 and Sample & Hold Amplifier SC-2040, has been used to measure engine variables with a sampling frequency up to 10 kHz. An AVL gravimetric balance is used to measure fuel consumption in steady-state conditions to calibrate the injector flow rate. The engine control system has been replaced with a dSPACE© MicroAutobox equipment and a power conditioning unit. Such a system allows to control all the engine tasks and to customize the control laws. To guarantee the controllability and reproducibility of the transient maneuvers, both throttle valve and engine speed are controlled through an AVL PUMA engine automation tool (see Fig. 2).

The exhaust AFR has been sensed by an ETAS Lambda Meter LA4, equipped with a Bosch LSU 4.2 UEGO sensor. This latter sensor has been placed right after the exhaust valve of the first cylinder.

This choice allows to remove the dynamic effects induced by gas transport and mixing phenomena occurring in the exhaust pipes. Also non predictable effects generated by cylinder-to-cylinder unbalance due to uneven processes such as air breathing, thermal state and fuel injection can be neglected. Therefore, the time shift between injection timing and oxygen sensor measurement mostly accounts

for the intake and exhaust valve phasing. As mentioned before, the time delay could represent a significant problem for control applications (Powell et al., 1998).

5. TRAINING AND TEST DATA

The training and test sets have been generated by running the engine on the test bench in transient conditions. In order to span most of the engine operating region, perturbations on throttle and load torque have been imposed during the transients. Fast throttle maneuvers, with large opening-closing profiles and variable engine speed set points, are generated off-line and assigned through the bench controller to engine and dyno, respectively (see Fig. 2). Such an approach also allows exciting the wall wetting dynamics without being influenced by a dominant frequency. Furthermore, in order to excite the high frequency dynamics of the manifold wall fuel film, a uniform random perturbation has been added to the injection base time, limiting the gain in the range +/- 15 % of the nominal fuel injection.

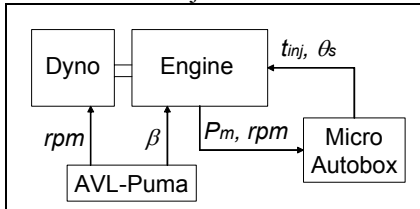


Fig. 2. Lay-out of the experimental plant. β = throttle opening, θ_s = spark advance, t_{inj} = injection time.

Fig. 3 shows the measured signals of throttle opening (a), engine speed (b), manifold pressure (c), injected fuel (d) and AFR (e) used as training-data (Set A). The throttle opening transient shown in Fig. 3 (a) allows exciting the filling-emptying dynamics of the intake manifold and the engine speed dynamics, as a consequence of both engine breathing and the energy balance between engine and load torque. Fig. 3 (b) and Fig. 3 (c) indicate that the transient spans most of the engine operating domain with engine speed and manifold pressure ranging from 1000 to 3000 rpm and from low to high load, respectively. The variation of manifold pressure and engine speed affects the intake air flow rate and consequently the amount of fuel to be injected to meet the target AFR. The injected fuel transient (see Fig. 3 (d)), commanded by the ECS, excites the wall wetting dynamics, which in turn influences the in-cylinder AFR and the engine torque delivery in a broad frequency range.

Fig. 4 shows the time histories of throttle opening, engine speed, manifold pressure, injected fuel and air fuel ratio, measured for the test-set (SET B). SET B has been obtained imposing square wave throttle maneuvers (Fig. 4 a) to excite the highest frequencies of the air dynamics, while keeping the engine speed constant (Fig. 4 b) and removing the fuel pulse random perturbation. Fig. 4 (d) and (e) evidence that the resulting step variations of injected fuel generate wide lean/rich spikes of AFR, due to uncompensated effects of wall wetting dynamics during abrupt throttle opening/closing transients. Such features make SET B suitable as test data-set since RNN accuracy

in predicting high frequency dynamic response is demanded. Moreover, the sharp variations in engine load (i.e. p_{man}), obtained via stepwise throttle opening, allow to identify the AFR delay. Thus, SET B is also very suitable to assess the ability of RNN in understanding the pure time delay.

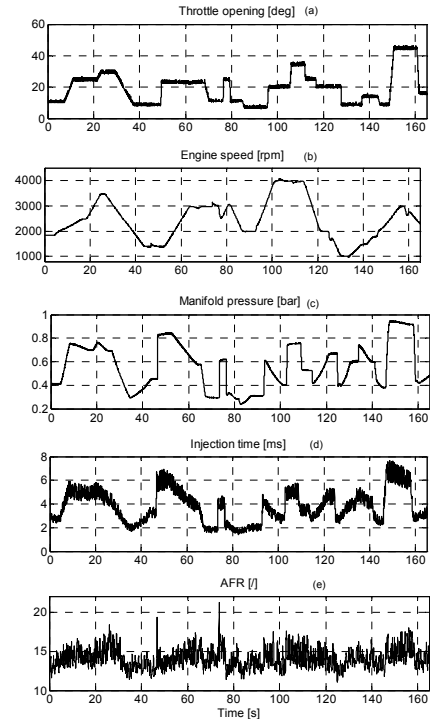


Fig. 3. Training data-set (SET A).

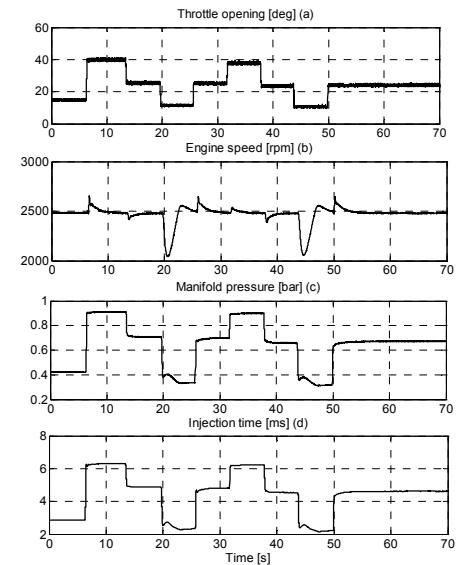


Fig. 4. Test data-set (SET B).

6. RESULTS

6.1 RNN estimator

A Forward RNN Model (FRNNM) of AFR dynamics was identified considering an NOE structure consisting of 12 hidden nodes, with a lag space $n = 2$ and $m = 5$. Following the indications provided by (Sorrentino et al., 2007), the AFR signal was back-shifted by a time delay corresponding to 5π crank-shaft interval. The latter value

was increased with respect to the value addressed in (Sorrentino et al., 2007) in order to better take into account, besides the pure time delay due to engine cycle, other delaying effects, such as: injection actuation; unsteadiness of gas flowing through the measuring section; mixing with residual gas present in the pipe from the previous cycle.

The accuracy of the developed FRNNM is demonstrated by the small discrepancies between measured and predicted AFR, as shown in Figures 5-8. Particularly, Fig. 7 and Fig. 8 show that the delay removal from the AFR signal enables the FRNNM to very well capture AFR dynamics in both rich and lean transients.

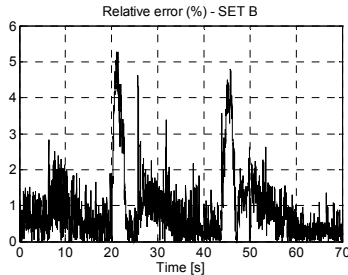


Fig. 5. Trajectories of relative error between measured and predicted AFR (SET B).

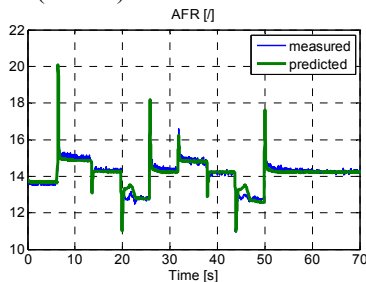


Fig. 6. Trajectories of measured and predicted AFR (SET B).

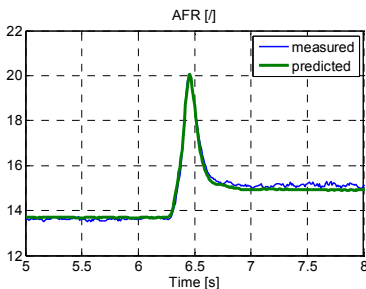


Fig. 7. Trajectories of measured and predicted AFR (SET B, time window [5, 8]).

6.1 RNN controller

In a previous paper (Arsie et al., 2004) it was discussed how an RNN-based controller of AFR excursion can be developed by training a network simulating inverse AFR dynamics. The general form of such an Inverse RNN Model (IRNNM) can be derived by inverting Eq. (3):

$$\hat{t}_{inj}(t-1, \theta_2) = G[AFR(t), \hat{t}_{inj}(t-2, \theta_2), \dots, \hat{t}_{inj}(t-m, \theta_2), x(t-1), \dots, x(t-m)] \quad (5)$$

Therefore, the IRNNM training task is performed almost in the same way as for the FRNNM, with the only difference that control and output variables are inverted. It is worth noting that past AFR values in Eq. (5) are not

included (whereas in Eq. (3) they are), since this controller is conceived in such a way as to perform open-loop fuel compensation.

Fig. 9 shows a comparison between experimental and simulated injection time, which confirms the high accuracy guaranteed by RNN in reproducing inverse AFR dynamics also. It is worth mentioning here that even the IRNNM was trained considering an AFR signal depurated of measuring delay. After the offline development, the IRNNM was embedded into dSPACE© MicroAutobox by replacing the actual AFR value (i.e. $AFR(t)$) by the desired value (i.e. $AFR_{des} = 14.67$), resulting in the following RNN controller:

$$\hat{t}_{inj}(t-1, \theta_2) = G[AFR_{des}, \hat{t}_{inj}(t-2, \theta_2), \dots, \hat{t}_{inj}(t-m, \theta_2), x(t-1), \dots, x(t-m)] \quad (6)$$

Fig. 10 shows the controlled AFR trajectory versus time. It can be seen how the online implementation of the IRNNM guarantees to satisfactorily limit AFR excursions within $\pm 5\%$ of the stoichiometric value, thus confirming the suitability of the proposed RNN-based controller.

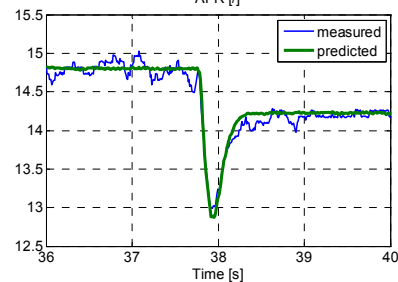


Fig. 8. Trajectories of measured and predicted AFR (SET B, time window [36, 40]).

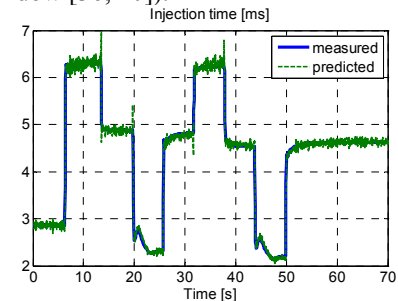


Fig. 9. Trajectories of measured and predicted injection time (SET B).

7. CONCLUSIONS

Recurrent Neural Network models have been developed to simulate both forward and inverse AFR dynamics.

Training and test data sets have been derived from experimental data obtained by imposing throttle and load perturbations. To enhance RNN generalization, the input variables have been uncorrelated by perturbing the fuel injection around stoichiometry.

The removal of a 5π delay from the measured AFR signal was proven to be necessary to ensure accurate prediction of AFR dynamics in correspondence of both rich and lean transients.

In the validation phase, the comparison between simulated and experimental transients indicated that AFR predicted by the RNN estimator (FRNNM) follows the reference

trajectory without any significant delay, thus proving that the RNN dynamic behavior is satisfactorily close to the real system dynamics.

Online implementation of RNN was accomplished by developing an inverse model (IRNNM) that is suitable for real-time control of AFR. Experimental test of the IRNNM controller, embedded in the framework of a dSPACE® MicroAutobox control unit, confirmed the great potential of RNN for limiting AFR excursions from stoichiometry.

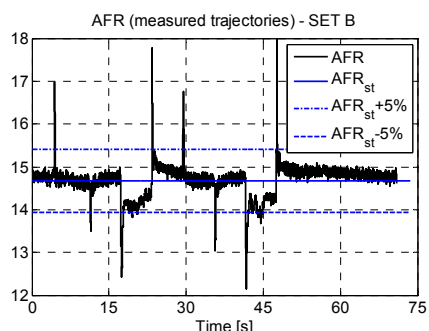


Fig. 10. Experimental trajectory of AFR controlled by means of the IRNNM compensator (i.e. Eq. 6).

REFERENCES

- Aquino, C.F., 1981, "Transient A/F Control Characteristics of the 5 Liter Central Fuel Injection Engine", SAE paper 810494.
- Arsie, I., Pianese, C., Sorrentino, M., 2007, "A Neural Network Air-Fuel Ratio Estimator for Control and Diagnostics in Spark-Ignited Engines", Proceedings of the Fifth IFAC Symposium on Advances in Automotive Control, Monterey (CA, USA) August, 20-22, 2007.
- Arsie, I., Marotta, M.M., Pianese, C., Sorrentino, M., 2006a, "Experimental Validation of a Neural Network Based A/F Virtual Sensor for SI Engine Control", SAE paper 2006-01-1351.
- Arsie, I., Pianese, C., Sorrentino, M., 2004, "Nonlinear Recurrent Neural Networks for Air Fuel Ratio Control in SI engines", SAE paper 2004-01-1364.
- Arsie, I., Pianese, C., Sorrentino, M., 2006, "A procedure to enhance identification of recurrent neural networks for simulating air-fuel ratio dynamics in SI engines", Engineering Applications of Artificial Intelligence 19 (1), pp. 65-77.
- Arsie, I., Pianese, C., Rizzo, G., Cioffi, V., 2003, "An Adaptive Estimator of Fuel Film Dynamics in the Intake Port of a Spark Ignition Engine", Control Engineering Practice, vol. 11, no. 3, pp. 303-309.
- Capriglione, D., Liguori, C., Pianese, C., Pietrosanto, A., 2003, "On-line Sensor Fault Detection Isolation, and Accomodation in Automotive Engines", IEEE Transactions on Instrumentation and Measurement, Vol. 52, No. 4, pp. 1182-1189.
- Choi, S.B., Hedrick, J.K., "An Observer-Based Controller Design Method for Improving Air/Fuel Characteristics of Spark Ignition Engines", IEEE Transactions on Control Systems Technology, Vol.6, No.3, May 1998.
- Colin, G., Chamailard, Y., Bloch, G., Corde, G., 2007, "Neural Control of Fast Nonlinear Systems Application to a Turbocharged SI engine with VCT", IEEE Trans. on Neural Networks, Vol. 18, No.4, July 2007.
- Dovifaaz, X., Ouladsine, M., Rachid, A., 1999, "Optimal Control of a Turbocharged Diesel Engine Using Neural Network", Proceedings of the 14th IFAC World Congress, IFAC-8b-009, Beijing, China, July 5-9, 1999.
- Haykin, S., 1999, Neural Networks, Prentice Hall.
- Hendricks, E., Sorenson, S.C., 1991, "SI Engine Controls and Mean Value Engine Modeling", SAE Paper 910258.
- Kolmogorov A..N. (1965), On the Representation of Continuous Functions of Many Variables by Superposition of Continuous Functions of One Variable and Addition, Amer. Math. Society Translations, 28, pp. 55-59, 1965.
- Locatelli, M., Alfieri, E., Onder C. H., Geering, H.P., 2006 "Identification of the Relevant Parameters of the Wall-Wetting System by Extended Kalman Filter", Control Engineering Practice, Volume: 14, Issue: 3, March, 2006, pp. 235-241.
- Maloney, P. J., "A Production Wide-Range AFR - Response Diagnostic Algorithm for Direct-Injection Gasoline Application", SAE Paper 2001-01-0558, 2001.
- Nørsgaard, M., Ravn, O., Poulsen, N.L., Hansen, L.K., 2000, Neural Networks for Modelling and Control of Dynamic Systems, Springer-Verlag.
- Onder, C. H., Roduner, C. A., Geering, H. P., "Model Identification for the A/F Path of an SI Engine", SAE Paper 970612, 1997.
- Ortmann, S., Glesner, M., Rychetsky, M., Tubetti, P., Morra, G., 1998, "Engine Knock Estimation Using Neural Networks based on a Real-World Database", SAE Paper 980513.
- Patterson, D.W., 1995, Artificial Neural Networks – Theory and Applications, Prentice Hall.
- Powell, J.D., Fekete, N.P., Chang, C.F., 1998, "Observer-Based Air-Fuel Ratio Control", IEEE Transactions on Control Systems, vol. 18, no. 5, pp. 72-83.
- Shayler, P.J., Goodman, M.S., Ma, T., 1996, "Transient Air/Fuel Ratio Control of an S.I. Engine Using Neural Networks", SAE Paper 960326.
- Tan, Y., Saif, M., 2000, "Neural-networks-based nonlinear dynamic modeling for automotive engines", Neurocomputing, vol. 30, pp. 129-142.
- Turin, R.C., Geering, H.P., 1994, "Model-Based Adaptive Fuel Control in an SI Engine", SAE Paper 940374.
- Vigild, C.W., Andersen, K.P.H., Hendricks, E., 1999, "Towards Robust H-infinity Control of an SI Engine's Air/Fuel Ratio", SAE Paper 1999-01-0854.
- Yasuri, Y., Shusuke, A., Ueno, M., Yoshihisa, I., 2000, "Secondary O2 Feedback Using Prediction and Identification Type Sliding Mode Control", SAE Paper no. 2000-01-0936.
- Yoo, I.K., Upadhyay, D., Rizzoni, G., 1999, "A Control-Oriented Carbon Canister Model", SAE Paper 1999-01-1103.